Inorganic Chemistry

Article

pubs.acs.org/IC

Temperature and Pressure Effects on C–H Abstraction Reactions Involving Compound I and II Mimics in Aqueous Solution

Maria Oszajca,[†,‡] Alicja Franke,[‡] Agnieszka Drzewiecka-Matuszek,[§] Małgorzata Brindell,[†] Grażyna Stochel,*[,†] and Rudi van Eldik*[,†,‡]

[†]Faculty of Chemistry, Jagiellonian University, Ingardena 3, 30-060 Krakow, Poland

[‡]Department of Chemistry and Pharmacy, University of Erlangen–Nuremberg, Egerlandstrasse 1, 91058 Erlangen, Germany

[§]Jerzy Haber Institute of Catalysis and Surface Chemistry, Polish Academy of Sciences, Niezapominajek 8, 30-239 Krakow, Poland

Supporting Information

ABSTRACT: The presented results cover a comparative mechanistic study on the reactivity of compound (Cpd) I and II mimics of a water-soluble iron(III) porphyrin, [*meso*-tetrakis(2,4,6-trimethyl-3-sulfonatophenyl)porphinato]iron(III), Fe^{III}(TMPS). The acidity of the aqueous medium strongly controls the chemical nature and stability of the high-valent iron(IV) oxo species. Reactivity studies were performed at pH 5 and 10, where the Cpd I and II mimics are stabilized as the sole oxidizing species, respectively. The contributions of $\Delta H^{‡}$ and $\Delta S^{‡}$ to the free energy of activation ($\Delta G^{‡}$) for the oxidation of 4-methoxybenzaldehyde (4-MB-ald), 4-methoxybenzyl alcohol (4-MB-alc), and 1-phenylethanol (1-PhEtOH) by the Cpd I and II mimics were determined. The relatively large contribution of the $\Delta H^{‡}$ term in comparison to the $-T\Delta S^{‡}$ term to $\Delta G^{‡}$ for reactions involving the Cpd II mimic indicates that the oxidation of selected substrates by this oxidizing species is clearly an enthalpy-controlled process. In contrast, different results were found for reactions with application of the Cpd I mimic. Depending on the nature of the substrate, the reaction at room temperature can be entropy-controlled, as found for the oxidation of 4-MB-alc, or enthalpy-controlled, as found for 1-PhEtOH. Importantly, for the first time, activation volumes ($\Delta V^{‡}$) for the oxidation of selected substrates by both reactive intermediates could be determined. Positive values of $\Delta V^{‡}$ were found for reactions with the Cpd II mimic and slightly negative ones for reactions with the Cpd II mimic. The results are discussed in the context of the oxidation mechanism conducted by the Cpd I and II mimics.

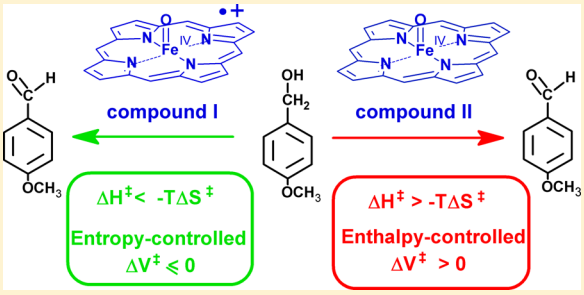

INTRODUCTION

Cytochrome P-450 constitutes a large family of enzymes that are able to catalyze the insertion of oxygen into chemically versatile organic molecules. Direct studies on the reactivity of high-valent iron(IV) oxo intermediates [viz. compounds (Cpds) I and II] involved in the catalytic cycle of the enzyme are often hampered because of difficulties in the detection and stabilization of these reactive species. The application of synthetic iron porphyrin models is a bountiful approach, giving information on different factors that influence the reaction mechanism and chemoselectivity of the reactive intermediates in oxygenation reactions.[1−7] Theoretical calculations that examine the reaction mechanism on the basis of calculated activation energy E_a values provide an additional source of information to the overall mechanistic picture.[8−12] The theoretical approach is based on the assumption that substrate oxidation reactions involving Cpds I and II are enthalpy-controlled processes; i.e., the contribution of the activation entropy to the free energy of activation should be negligible in comparison to that of the activation enthalpy. However, studies performed by Takahashi et al.[13] demonstrated nicely that such an assumption can sometimes be misleading because the entropy term may indeed control the chemoselectivity of cyclohexene oxygenation. A large contribution of the entropy term ($-T\Delta S^{‡}$) to $\Delta G^{‡}$ found for both epoxidation and allylic hydroxylation of cyclohexene indicates that in such cases $\Delta G^{‡}$ instead of E_a should be used to predict reaction mechanisms. In addition, a comparative study on the activation parameters for epoxidation and the C–H abstraction reactions catalyzed by Cpd I and II mimics pointed out that the chemical nature of both the reactive intermediate and substrate can influence the relative impact of $\Delta H^{‡}$ and $\Delta S^{‡}$ on the $\Delta G^{‡}$ value.[14] The free-energy barrier governed more by the $-T\Delta S^{‡}$ term than the $\Delta H^{‡}$ term has also been reported for hydrogen abstraction reactions by the *tert*-butoxyl radical and rhodium(II) tetramesitylporphyrin [(TMP)Rh$^{•}$].[15,16] Furthermore, it has also been shown that the oxidation of benzyl alcohol by nonheme high-valent iron oxo complexes is entropy-controlled, whereas the oxidation by porphyrin cation-radical iron(IV) oxo species is enthalpy-controlled.[17]

Received: October 10, 2013
Published: January 6, 2014

   dx.doi.org/10.1021/ic402567h | *Inorg. Chem.* 2014, 53, 2848–2857

These cases indicate that the commonly assumed correlation of the rate constant with C−H bond strength (bond dissociation energy, BDE) may not be valid in some cases because a large contribution of $\Delta S^{\ddagger}$ to $\Delta G^{\ddagger}$ leads to a significant temperature dependence of the activation barrier. This is especially apparent for oxidation reactions that involve substrates possessing weak C−H bonds for which the determined activation energies did not vary significantly with C−H BDE and therefore the Evans−Polanyi equation appeared to be not relevant.[15] The meaningful contribution of the activation entropy to the oxygenation process indicates that the reaction mechanism and chemoselectivity of the reactive intermediates in biomimetic studies can be tuned by systematic variation of the temperature. This finding nicely correlates with the results shown by Song et al.,[3] who demonstrated that product distribution in cyclohexene oxidation (hydroxylation vs epoxidation) strongly depends on the reaction temperature when iron porphyrins with electron-donating substituents on the porphyrin rings were used as catalysts.

The above-presented considerations clearly underline the fact that the reaction mechanism and reactivity of high-valent iron(IV) oxo species strongly depend on such factors as the solvent,[18,19] axial ligands[19−21] or electronic nature of the porphyrin.[3,22] Because the activation parameters ($\Delta S^{\ddagger}$ and $\Delta H^{\ddagger}$) determined so far for substrate oxidation by Cpd I and II mimics concern exclusively the reactions carried out in organic media, we report here a study on the thermal activation parameters for the oxidation of selected substrates in aqueous solution. The application of nonaggregating synthetic iron porphyrin, [*meso*-tetrakis(2,4,6-trimethyl-3-sulfonatophenyl)-porphinato]iron(III), (TMPS)Fe^{III} (Scheme 1A), provided an ideal opportunity to perform a study on the mechanism of formation of Cpd I and II mimics and their reactivity/stability in an aqueous medium as a function of the pH.[23−25]

To examine the contribution of the activation enthalpy and activation entropy to the free energy of activation for the oxidation processes carried out by the two reactive intermediates, viz., Cpd I and II mimics, we explored the temperature dependence of their reactivity toward selected substrates. Because in aqueous solution the acidity of the medium strongly controls the chemical nature and stability of the high-valent iron(IV) oxo species, the reactivity study was performed at pH 5 and 10, where the Cpd I and II mimics are stabilized as the sole oxidizing species, respectively.[23,24]

Importantly, we were for the first time able to successfully determine values for the activation volume ($\Delta V^{\ddagger}$) for the oxidation of selected substrates (Scheme 1B) by both Cpd I and II mimics. As is well-known, the additional physical parameter of pressure adds another dimension to the mechanistic understanding of a broad array of (bio)inorganic processes, allowing analysis of the studied reactions in terms of volume changes along the reaction coordinate. However, as far as we know, mechanistic studies dealing with pressure-dependent kinetic measurements for the oxidation of unreactive substrates by iron(III) porphyrin activated peroxides have not been reported in the literature so far. This mainly results from the fact that the high-valent iron intermediates formed in the peroxo-shunt oxidation reactions are highly reactive species that cannot be sufficiently stabilized in order to perform appropriate pressure-dependent measurements. The system presented in this study together with the selection of appropriate reaction conditions allowed us for the first time to investigate pressure effects on the C−H abstraction reactions involving Cpd I and II mimics as oxidizing species. In order to obtain the activation volumes, we examined the kinetics of the reactions of both the high-valent oxoiron(IV) cation-radical porphyrin and high-valent oxoiron(IV) porphyrin with selected substrates as a function of the pressure. We strongly believe that this additional information can be very helpful in the elucidation of the underlying reaction mechanism and can provide new insight into the comprehension of mechanistic aspects that affect the reactivity of Cpd I and II mimics.

Scheme 1. (A) Structure of (TMPS)Fe^{III} and Its Reaction with *m*-CPBA To Produce Cpd I or II and (B) Structures of the Studied Substrates and Their Oxidation Products

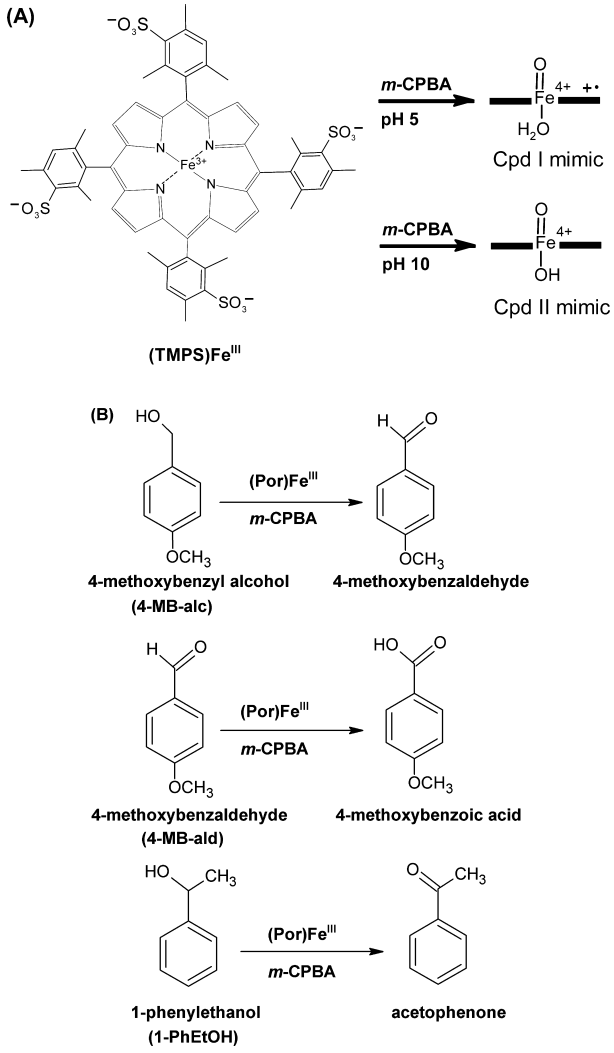

EXPERIMENTAL SECTION

Materials. All chemicals used in this study were of analytical reagent grade. The iron(III) porphyrin [*meso*-tetrakis(2,4,6-trimethyl-3-sulfonatophenyl)porphinato]iron(III) hydroxide (tetrasodium salt), Fe^{III}(TMPS)(OH) (>95%), was purchased from Frontier Scientific Inc. (Logan, UT) and used as received. *m*-Chloroperoxybenzoic acid (*m*-CPBA) was purchased from Acros Organic (75%) and purified by recrystallization from hexane (Note: pure *m*-CPBA is shock-sensitive and potentially explosive and can deflagrate; care is required while carrying out the reactions and during workup). Boric acid, sodium acetate, 4-methoxybenzyl alcohol (4-MB-alc; 98%), 4-methoxybenzaldehyde (4-MB-ald; >99%), and 1-phenylethanol (1-PhEtOH; 98%) were purchased from Sigma Aldrich and used as received. All solutions were prepared in deionized water.

dx.doi.org/10.1021/ic402567h | Inorg. Chem. 2014, 53, 2848−2857

Product Analysis. In order to analyze the oxidation products of selected substrates, *m*-CPBA (3×10^{-4} and 2×10^{-4} M for generation of Cpds I and II, respectively) was added to a 2×10^{-4} M porphyrin complex in an acetate buffer (pH 5.0), or a borate buffer (pH 10), for Cpds I and II, respectively. Subsequently, 4-MB-alc (20 mM), 4-MB-ald (6.2 mM), or 1-PhEtOH (30 mM) was added to the reaction solution. In the case of 4-MB-ald oxidation, the samples for product analysis were prepared under inert conditions because it was found that the presence of oxygen can influence the oxidation reactions on a longer time scale. This was not the case for the oxidation of alcohols. After completion of the oxidation reactions, the obtained reaction mixtures were analyzed by a Perkin-Elmer high-performance liquid chromatography (HPLC) Chromera system. A Brownlee Validated AQ C18 5 μm, 250 × 4.6 mm column was employed for HPLC separation, and H_2O (50%) and CH_3CN (50%) or 0.01% trifluoroacetic acid in H_2O (50%) and CH_3CN (50%) were used as a mobile phase at a flow rate of 1 mL min^{-1}. The chemical identities of the obtained oxidation products were determined by a comparison of their characteristic UV spectra with those of known authentic samples. The amounts of the oxidation products were derived from the standard curves of known authentic samples. The resulting product yields were calculated based on the amount of added *m*-CPBA. An accurate concentration of the latter was determined by iodometric titration.

Kinetic Measurements. Ambient-pressure stopped-flow measurements were performed on a thermostatted (±0.1 °C) Applied Photophysics SX20 stopped-flow apparatus equipped with a sequential mixing mode. The kinetics of the reaction of the high-valent iron species with selected substrates was studied under pseudo-first-order conditions. In a typical experiment, buffered solutions of the porphyrin complex were rapidly mixed with appropriately concentrated solutions of *m*-CPBA in the first mixing drive. After a defined delay period, the aged solution was mixed with an organic substrate in the second mixing drive, and the reaction was followed spectrophotometrically. Depending on the selected reaction conditions, $(TMPS^{\bullet+})Fe^{IV}{=}O$ or $(TMPS)Fe^{IV}{=}O$ was formed at pH 5.0 or 10.0, respectively. High-pressure stopped-flow experiments were performed in the pressure range of 10−130 MPa on a custom-built apparatus.[26,27] *OLIS KINFIT* software (Bogart, GA, 1989) was used for analysis of the kinetic traces.

Calculation of the C−H BDEs. A quantum-chemical method based on density functional theory with the nonlocal B3LYP (Becke, three-parameter, Lee−Yang−Parr) functional[28−33] was applied to calculate the reorganization energies of the 4-MB-alc, 4-MB-ald, and 1-PhEtOH radicals. These energies were obtained as an energy difference between their geometries as in the substrate (no relaxation after hydrogen removal) and in the fully relaxed geometry of the radicals, following the concepts introduced by Shaik and co-workers.[34] The presented results were obtained with *TURBOMOLE*, version 6.3.[35]

RESULTS AND DISCUSSION

Generation of Reactive Intermediates. The $Fe^{III}(TMPS)$ complex is known to be a good biomimetic of heme enzymes, which because of its high water solubility provides a unique opportunity to examine the oxidizing ability of the Cpd I and II mimics for selected inert substrates under aqueous conditions. The $Fe^{III}(TMPS)$ complex can exist either as the six-coordinate diaqua-ligated $[(TMPS)Fe^{III}(H_2O)_2]^{3-}$ or the five-coordinate monohydroxo-ligated $[(TMPS)Fe^{III}(OH)]^{4-}$ species (pK_a = 6.8) depending on the pH of the solution.[36,37] As is known from earlier studies, the acidity of the reaction medium strongly affects the catalytic activity of water-soluble iron(III) porphyrins, which is ascribed to pH-dependent changes in the iron(III) porphyrin speciation and its electrochemical properties.[6,23,38] Accordingly, a gradual change in the nature of the product formed upon the oxidation of $Fe^{III}(TMPS)$ from the oxoiron(IV) porphyrin cation radical $[(TMPS^{\bullet+})Fe^{IV}{=}O(H_2O)]^{3-}$ at low pH to the oxoiron(IV) porphyrin $[(TMPS)Fe^{IV}{=}O(OH)]^{5-}$ at high pH was observed.[23] These observations correlate with the pH dependence of $E^{\circ\prime}$ for the electrochemical oxidation of $Fe^{III}(TMPS)$ in aqueous solution, as reflected by pH-dependent changes in the relative position of $E^{\circ\prime}(Fe^{IV}/Fe^{III})$ and $E^{\circ\prime}(P^{\bullet+}/P)$.[24] In the context of chemical oxidation involving O−O bond cleavage of coordinated peroxide, the dependence of $E^{\circ\prime}$ on the pH implies that heterolysis of the O−O bond should be favored in the pH range 4−7, in which $E^{\circ\prime}(Fe^{IV}/Fe^{III}) \approx E^{\circ\prime}(P^{\bullet+}/P)$ (Scheme 2, routes A and C). As a result of this, thermodynamically stabilized $(TMPS^{\bullet+})Fe^{IV}{=}O(H_2O)$ species are formed under such conditions. In contrast, at pH >7, where $E^{\circ\prime}(Fe^{IV}/Fe^{III})$ has lower values than $E^{\circ\prime}(P^{\bullet+}/P)$, homolysis of the O−O bond is the favored process (Scheme 2, routes B and D), leading to the formation of $[(TMPS)Fe^{IV}{=}O(OH)]^{5-}$. One should, however, keep in mind that the mode of O−O bond cleavage depends also on the oxidative power of the applied oxidant. Therefore, for a strong oxidant such as *m*-CPBA, for which $E^{\circ\prime}$ exceeds both $E^{\circ\prime}(Fe^{IV}/Fe^{III})$ and $E^{\circ\prime}(P^{\bullet+}/P)$, the heterolytic O−O bond cleavage (two-electron oxidation) may take place even at pH >7 (Scheme 2, routes B and C). However, the product formed [oxoiron(IV) porphyrin cation radical] is not thermodynamically stable under basic conditions and immediately decays via a comproportionation pathway (Scheme 2) or because of the presence of other redox-active species in the studied system. As a consequence, the $[(TMPS)Fe^{IV}{=}O(OH)]^{5-}$ species is observed as the sole product under such conditions.

Scheme 2. Schematic Representation of the Formation of $(TMPS^{\bullet+})Fe^{IV}{=}O(H_2O)$ and $(TMPS)Fe^{IV}{=}O(OH)$ under Acidic (pH 5) and Basic (pH 10) Conditions, Respectively

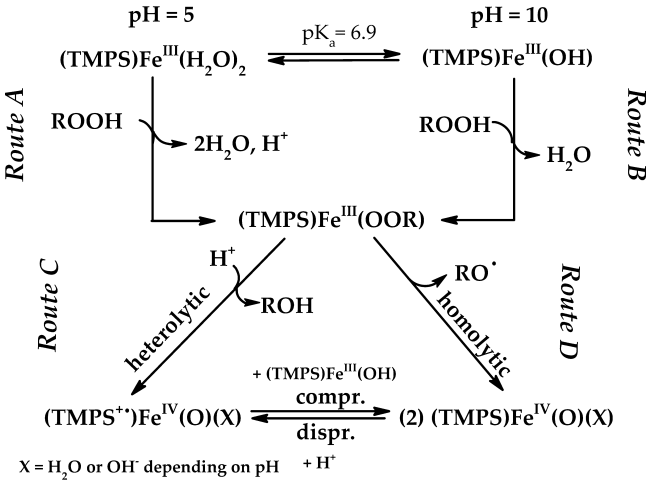

This means that the nature of the high-valent oxo species being formed can be tuned and stabilized by changing the pH. Therefore, to compare the reactivity of synthetic equivalents of Cpds I and II in aqueous solution, we generated in situ these species through the oxidation of $Fe^{III}(TMPS)$ by *m*-CPBA at pH 5.0 and 10.0, where the Cpd I and II mimics were stabilized as the sole oxidizing species, respectively.[23]

The reaction of $Fe^{III}(TMPS)$ with *m*-CPBA at pH 5.0 was followed by the application of stopped-flow spectrophotometry. The time-resolved spectral changes indicated fast (in ca. 50 ms at 20 °C) formation of a new species with decreased intensity of the Soret band at 400 nm and an emerging broad band with a maximum around 667 nm, typical for formation of the

dx.doi.org/10.1021/ic402567h | Inorg. Chem. 2014, 53, 2848−2857

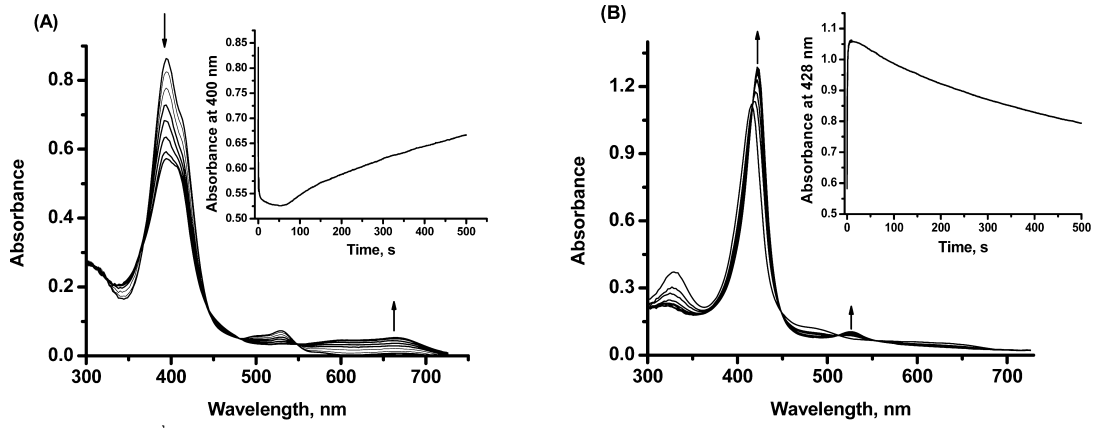

Figure 1. (A) UV−vis spectral changes observed for the reaction of (TMPS)Fe^{III} with *m*-CPBA at pH 5.0. Inset: Kinetic trace recorded for this reaction at the Soret band displaying the subsequent slow decomposition of $(TMPS^{\bullet+})Fe^{IV}{=}O(H_2O)$. Experimental conditions: [acetate buffer] = 0.05 M, pH 5, $[(TMPS)Fe^{III}(H_2O)_2] = 1 \times 10^{-5}$ M, [*m*-CPBA] = 1.5×10^{-5} M, T = 20 °C. (B) UV−vis spectral changes observed for the reaction of (TMPS)Fe^{III} with *m*-CPBA at pH 10.0. Inset: Kinetic trace recorded for this reaction at the Soret band displaying the subsequent slow decomposition of $(TMPS)Fe^{IV}{=}O(OH)$. Experimental conditions: [borate buffer] = 0.05 M, pH 10.0, $[(TMPS)Fe^{III}(OH)] = 1 \times 10^{-5}$ M, [*m*-CPBA] = 0.5×10^{-5} M, T = 5 °C.

iron(IV) oxo porphyrin π-cation radical (model for Cpd I;[23,39] see Figure 1A).

The complete transformation of the starting $[(TMPS)Fe^{III}(H_2O)_2]^{3-}$ complex to $[(TMPS^{\bullet+})Fe^{IV}{=}O(H_2O)]^{3-}$ required a slight excess of oxidant over the catalyst. The Cpd I analogue, however, is unstable and undergoes a slow subsequent reduction to the starting complex (see inset Figure 1A). The analogous reaction carried out at pH 10.0 resulted in accumulation of the one-electron-oxidized form of $[(TMPS)Fe^{III}(OH)]^{4-}$, assigned to iron(IV) oxo (model for Cpd II) with a characteristic Soret band maximum at 420 nm and a low-intensity band at 524 nm (Figure 1B).[23,40] The iron(IV) oxo species was described as a six-coordinate complex with a OH^- ligand in the position trans to the oxo group.[25] As shown previously,[25] the $[(TMPS)Fe^{IV}{=}O(OH)]^{5-}$ intermediate that is formed under such selected reaction conditions represents the *sole* oxidizing species in the reaction medium. This means that the latter species is not involved with $[(TMPS)Fe^{III}(OH)]^{3-}$ and $[(TMPS^{\bullet+})Fe^{IV}{=}O(H_2O)]^{3-}$ in disproportionation/comproportionation equilibria, as was observed for other iron porphyrin systems in organic solvents.[41] The $[(TMPS)Fe^{IV}{=}O(OH)]^{5-}$ species is not stable in aqueous solution and undergoes slow conversion to the starting $[(TMPS)Fe^{III}(OH)]^{4-}$ complex (see the inset in Figure 1B).

Mechanistic Studies on Substrate Oxidation. Because the Cpd I and II models can be selectively produced and stabilized at selected pH values and lower temperature (5 °C), it provided an exceptional opportunity to compare the influence of the temperature and pressure on the direct oxidation reactions of selected organic substrates by these oxidizing species in aqueous solution. In the course of this study, three different substrates were used, viz., 4-MB-alc, 4-MB-ald, and 1-PhEtOH.

In order to determine the chemical nature and yield of the oxidation products formed, the reaction mixtures consisting of (TMPS)Fe^{III} catalyst, *m*-CPBA, and selected substrates were subjected to product analysis with the use of HPLC (see the Experimental Section for more details regarding the analytical procedure). It was found that 4-methoxybenzoic acid (55 ± 5% for Cpd I and 32 ± 11% for Cpd II), 4-MB-ald (48 ± 4% for Cpd I and 34 ± 3% for Cpd II), and acetophenone (10 ± 2% for Cpd I and 6 ± 1% for Cpd II) were formed as major products in the oxidation reactions of 4-MB-ald, 4-MB-alc, and 1-PhEtOH, respectively (see Scheme 1B for the structures of the oxidation products). It should be noted that any significant side reactivity leading to the formation of side oxidation or overoxidation products was not observed for the oxidation of alcohols. However, in the case of aldehyde oxidation, it was found that the presence of oxygen could affect the oxidation reactions on a longer time scale, leading to a very high yield of 4-methoxybenzoic acid. This can be an indication that carbon radicals of 4-MB-ald formed via C−H abstraction may escape from the solvent cage and be scavenged by O_2 to give the corresponding peroxyl radicals, which undergo further reactions.[42] In this context, the samples for product analysis involving 4-MB-ald as the substrate were prepared under inert conditions.

The obtained product yields were calculated based on the quantity of the added oxidant, not with respect to the quantity of generated iron(IV) oxo species.[17,41] Therefore, the presented results reflect the efficiency of the conversion of (TMPS)Fe^{III} to the active species, i.e., Cpd I or II mimic, under the selected reaction conditions. As we reported previously,[25] the complete conversion of (TMPS)Fe^{III} to the Cpd I or II mimic requires an excess of oxidant over the catalyst, but this, in turn, can lead to fast destruction of the porphyrin. In the case of the oxidation of 1-PhEtOH, relatively low product yields were obtained for both Cpd I and II mimics. Because product analysis involving this substrate revealed that, aside from acetophenone, no other oxidation products were formed and only nonreacted substrate remained in the reaction mixture, the low product yields obtained for the oxidation of 1-PhEtOH clearly reflect the low reactivity of this substrate toward Cpds I and II, as was also confirmed in subsequent kinetic studies.

The kinetics of substrate oxidation was examined by following the depletion of in situ generated intermediates, $[(TMPS^{\bullet+})Fe^{IV}{=}O(H_2O)]^{3-}$ or $[(TMPS)Fe^{IV}{=}O(OH)]^{5-}$, upon the addition of different concentrations of the substrates. In all cases, selection of the appropriate reaction conditions[25] allowed one to observe almost complete re-formation of the starting iron(III) porphyrin complex (see, for example, Figure

dx.doi.org/10.1021/ic402567h | Inorg. Chem. 2014, 53, 2848−2857

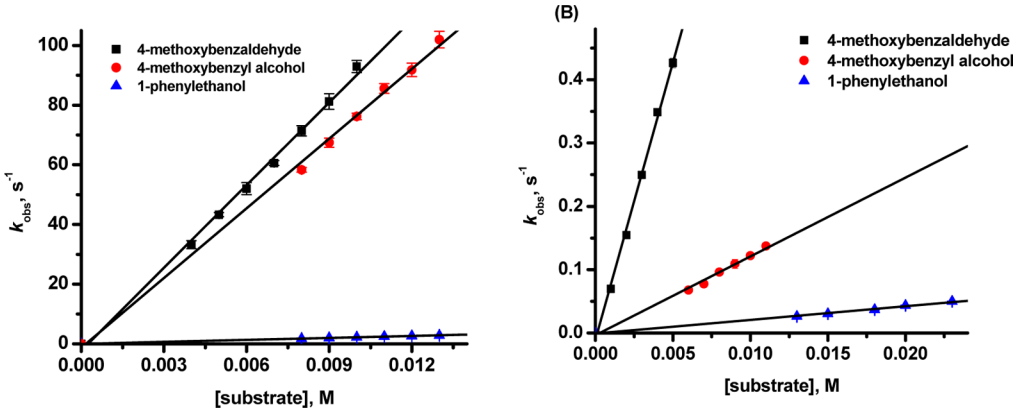

Figure 2. Plots of k_{obs} versus substrate concentration: squares, 4-MB-ald; circles, 4-MB-alc; triangles, 1-PhEtOH. (A) Reaction of model Cpd I with various substrates. Experimental conditions: $[(TMPS)Fe^{III}(H_2O)_2] = 5 \times 10^{-6}$ M, [*m*-CPBA] = (3.0−3.5) × 10^{-6} M, [acetate buffer] = 0.1 M, pH 5.0, T = 5 °C. (B) Reaction of model Cpd II with various substrates. Experimental conditions: $[(TMPS)Fe^{III}(OH)] = (3.7–5) \times 10^{-6}$ M, [*m*-CPBA] = (1.5−2.25) × 10^{-6} M, [borate buffer] = 0.1 M, pH 10.0, T = 5 °C.

Table 1. Rate Constants and Activation Parameters for the Oxidation of Selected Substrates by Cpds I and II, as Well as Calculated C−H BDEs of the Substrates Used in This Study

	k [M^{-1} s^{-1}], at 5 °C	$\Delta H^{\ddagger}$ [kJ mol^{-1}]	$\Delta S^{\ddagger}$ [J mol^{-1} K^{-1}]	$\Delta V^{\ddagger}$ [cm^3 mol^{-1}]	$-T\Delta S^{\ddagger}$(5 °C) [kJ mol^{-1}]	$\Delta G^{\ddagger}$(5 °C) [kJ mol^{-1}]	BDE_{C-H} [kJ mol^{-1}]	D_{C-H}[a] [kJ mol^{-1}]
				Compound I				
1-PhEtOH	219 ± 2	33 ± 1	−80 ± 2	−2.3 ± 0.2	22.2 ± 0.5	55 ± 2	361.2	427.0
4-Mb-alc	7790 ± 173	22.4 ± 0.4	−89 ± 1	−2 ± 1	24.7 ± 0.3	47 ± 1	367.2	430.0
4-Mb-ald	9235 ± 219	24 ± 1	−80 ± 2		22.2 ± 0.5	46 ± 2	403.2	406.5
				Compound II				
1-PhEtOH	2.2 ± 0.1	52 ± 1	−51 ± 4	+16.6 ± 0.6	14 ± 1	66 ± 2	361.2	427.0
4-Mb-alc	12.4 ± 0.4	46 ± 1	−59 ± 3	+12.6 ± 1.2	16.4 ± 0.8	62 ± 2	367.2	430.0
4-Mb-ald	87.6 ± 2.3	45 ± 1	−45 ± 3	+9.9 ± 0.8	12.5 ± 0.8	57 ± 2	403.2	406.5

[a]Bond strength entity, D_{C-H}, defined as $D_{C-H} = BDE_{C-H} + |RE_R|$, where RE_R is the relaxation energy of the substrate radical.[34]

S1 in the Supporting Information, SI) after the addition of the selected substrate.

Because the oxidation of iron(III) porphyrin species by *m*-CPBA and subsequent reduction of the formed oxidizing species by selected substrates were relatively fast reactions, the kinetic studies were performed using a stopped-flow technique equipped with a double mixing drive. With the first mixing drive, the solution of the catalyst and *m*-CPBA was mixed in a volume ratio of 1:1 to generate $[(TMPS^{\bullet+})Fe^{IV}{=}O(H_2O)]^{3-}$ or $[(TMPS)Fe^{IV}{=}O(OH)]^{5-}$ depending on the selected pH. With the second mixing drive, after a defined delay period, the solution of the reactive intermediate generated in situ was mixed with the substrate solution and the oxidation reaction was followed spectrophotometrically. In order to avoid interference coming from initiation of the catalytic cycle by unconsumed oxidant, both high-valent iron oxo species were generated by the application of subequivalent amounts of *m*-CPBA with respect to the porphyrin catalyst.[25] Pseudo-first-order kinetic traces for reduction of the high-valent iron(IV) oxo species recorded at the appropriate wavelengths were fitted to a single-exponential function, and k_{obs} values for each reaction system were obtained. The reported pseudo-first-order rate constants are mean values of at least six kinetic runs, and the quoted uncertainties are based on standard deviations (Table S1 in the SI). In all cases, the dependence of k_{obs} on the substrate concentration showed a linear behavior without a meaningful intercept (Figure 2) and was used to determine the corresponding second-order rate constants (Table 1).

Under the selected reaction conditions, relatively high concentrations of substrate (>1 mM) were used. This is because a fast substrate oxidation is required to avoid interference of spontaneous decomposition of the reactive intermediates and initiation of the catalytic cycle.[25] The pseudo-first-order behavior of the recorded kinetic traces and linear dependence of k_{obs} on [substrate] indicate that secondary oxidation reactions can be ruled out.

A comparison of the second-order rate constants (k) for the oxidation of a particular substrate by the high-valent iron(IV) oxo species reveals much higher k values for the reactions involving Cpd I than Cpd II. This finding is not surprising because the outstanding oxidizing capability of model Cpd I in comparison to model Cpd II is well-known.[40,43] The significantly higher reactivity of 4-MB-alc and 4-MB-ald in comparison to that of 1-PhEtOH can be accounted for in terms of the presence of an electron-donating group in the para position of the benzyl substrate. The enhanced reactivity of *p*-CH_3O-substituted benzyl alcohol and benzaldehyde in the oxidation reactions has already been documented in the literature.[41,44]

Interestingly, the values of the rate constants obtained in the present study for the oxidation of 1-PhEtOH and 4-Mb-alc by both reactive intermediates are much higher than that reported by Pan and Newcomb[41] with the application of an iron(III) porphyrin catalyst possessing electron-withdrawing aryl substituents in an nonaqueous solvent. This is quite surprising in view of the fact that the reactivity studies performed on a series of meso-substituted metal−oxo porphyrins showed an increase

dx.doi.org/10.1021/ic402567h | Inorg. Chem. 2014, 53, 2848−2857

in the oxidative power of the oxoiron(IV) porphyrin π-cation-radical oxidants with increasing electron deficiency in the macrocyclic ligand.[45−47] A possible explanation for the observed discrepancy can involve solvent effects (organic solvent vs aqueous medium) or the fact that the reactive species in the latter studies, iron(IV) porphyrin cation radical, was formed via disproportionation of the porphyrin iron(IV) oxo species under selected reaction conditions.

The oxidation of alcohols and aldehydes by heme and nonheme iron(IV) oxo complexes proceeds by a two-electron process to yield the corresponding aldehydes and acids, respectively (Scheme 3).[17,42] The first reaction step, involving

Scheme 3. Suggested Mechanism for the Oxidation of Aldehyde (A) and Alcohol (B) by Cpd I, Including the Transition State for the Rate-Limiting Step

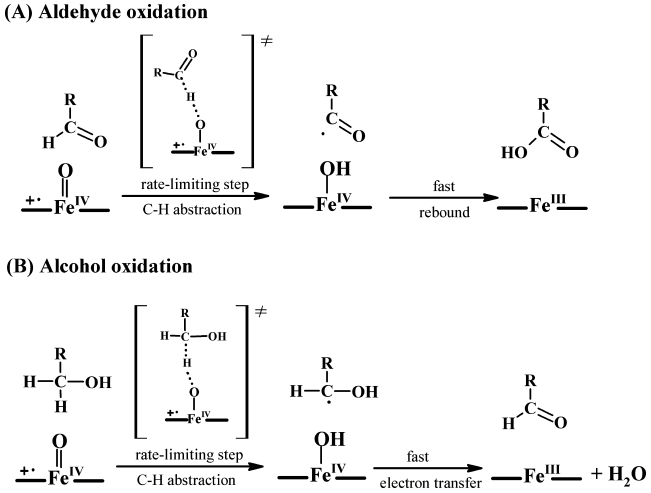

C−H hydrogen abstraction with the formation of a radical intermediate, is regarded as the rate-determining step in the overall oxidation process.[17,48] In hydroxylation reactions, radical formation is followed by a very fast displacement of OH from iron by the radical, the so-called "rebound" step.[12,49,50] However, in the case of alcohol oxidation, it has been shown that a dual-hydrogen abstraction process takes place instead of dehydration of the *gem*-diol intermediate (Scheme 3B).[17]

Because the values of the rate constants determined for substrate oxidation represent the rate-determining step (hydrogen abstraction), which is the same for all studied reactions, we can directly compare the activation parameters obtained for the oxidation reactions involving the Cpd I and II mimics.[17,42,48] The temperature dependence of k_{obs} for the oxidation of selected substrates was examined in the temperature range from 5 to 25 °C. At each temperature, at least six data points were acquired. The obtained data (Table S2 in the SI) enabled the construction of Eyring plots, as shown in Figure 3. From the slopes and intercepts of the obtained linear plots, the activation enthalpies ($\Delta H^{\ddagger}$) and activation entropies ($\Delta S^{\ddagger}$) were calculated, respectively (see Table 1).

In order to determine the influence of the pressure on the reactivity of each oxidizing intermediate toward the selected substrates, the oxidation reactions were studied over the pressure range 10−130 MPa at 5 °C. The reported rate constants at each pressure are the mean values of at least eight kinetic runs (Table S3 in the SI). The obtained linear dependence of ln(k) versus pressure allowed determination of

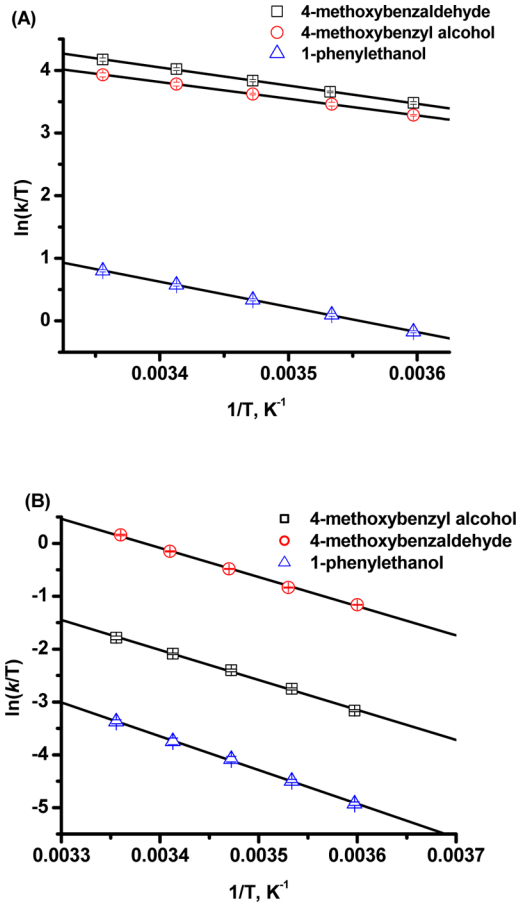

Figure 3. Eyring plots for substrate oxidation by (A) the Cpd I mimic ([acetate buffer] = 0.1 M; pH 5.0) and (B) the Cpd II mimic ([borate buffer] = 0.1 M; pH 10.0).

the activation volume (Figure 4). Because of the relatively high reaction rate for the oxidation of 4-Mb-ald by the Cpd I mimic and the limitation of the high-pressure instrument, determination of the $\Delta V^{\ddagger}$ value for this reaction was not possible. It is also important to note that $\Delta V^{\ddagger}$ for 4-Mb-alc oxidation by the Cpd I mimic is associated with high uncertainties because the reaction rate is close to the performance limits of the employed high-pressure stopped-flow instrument. The values of $\Delta H^{\ddagger}$, $\Delta S^{\ddagger}$, and $\Delta V^{\ddagger}$ listed in Table 1 are the mean values from at least two independent measurements.

It was previously shown that Cpd II is a rather sluggish oxidant in comparison to Cpd I.[14,40] This tendency is also reflected in the present study by the values of $\Delta H^{\ddagger}$ and $\Delta S^{\ddagger}$ determined for the oxidation of selected substrates and the corresponding values of the Gibbs free activation energy ($\Delta G^{\ddagger} = \Delta H^{\ddagger} - T\Delta S^{\ddagger}$). The difference between the values of $\Delta G^{\ddagger}$ obtained for the oxidation reactions involving the Cpd I and II mimics lies in the range of 11−15 kJ mol^{-1} depending on the substrate. This is in agreement with the results of similar studies performed in acetonitrile with the use of an Fe^{III}(TMP) complex as the catalyst, which showed that the free energy of activation for the reactions of the Cpd II mimic are around 9−11 kJ mol^{-1} higher than the corresponding values found for the Cpd I mimic.[14]

Analysis of the second-order rate constants listed in Table 1 for the Cpd I and II mimics reveals that both reactive species display the same trend in the reactivity toward the selected substrates, viz., 1-PhEtOH < 4-Mb-alc < 4-Mb-ald.

dx.doi.org/10.1021/ic402567h | Inorg. Chem. 2014, 53, 2848−2857

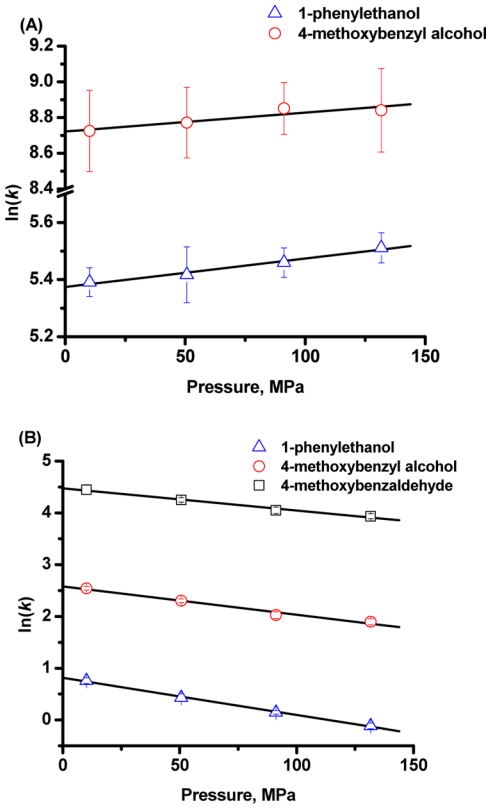

Figure 4. Plots of ln(k) versus pressure for the oxidation of various substrates by (A) the Cpd I mimic ([acetate buffer] = 0.1 M; pH 5.0; T = 5 °C) and (B) the Cpd II mimic ([borate buffer] = 0.1 M; pH 10.0; T = 5 °C).

Upon comparison of the values of k with the activation enthalpy ($\Delta H^{\ddagger}$) for the reactions of the Cpd II mimic, a correlation between the observed reactivity and $\Delta H^{\ddagger}$ can be found; i.e., the higher value of k corresponds to the lower value of $\Delta H^{\ddagger}$. The relatively small impact of the $-T\Delta S^{\ddagger}$ term on the free energy of activation for the reactions involving the Cpd II mimic indicates that the oxidation of selected substrates by this oxidizing species is clearly an enthalpy-controlled process. In contrast, the data found for the reaction of the Cpd I mimic with 4-Mb-alc or 4-Mb-ald show an almost comparable contribution from the activation entropy and activation enthalpy to the overall activation barrier ($\Delta G^{\ddagger}$), implying that the entropy effects play an essential role in the oxidation of these substrates. Similarly, although the oxidation reaction of 1-PhEtOH by the Cpd I mimic reveals a significant domination of the enthalpy term, the contribution of the activation entropy to $\Delta G^{\ddagger}$ appeared to be considerably larger than that found for the oxidation of this substrate by the Cpd II mimic. All observations are in line with the conclusions drawn from studies on the C−H abstraction reactions with the application of Fe^{III}(TMP) as the catalyst in an organic solvent, in which the oxidation of xanthene by the Cpd I mimic was shown to be an entropy-controlled process, whereas the oxidation of the same substrate by the Cpd II mimic appeared to be an enthalpy-controlled reaction.[14] On the other hand, studies on benzyl alcohol oxidation performed by Nam and co-workers showed a large contribution of the enthalpy term to $\Delta G^{\ddagger}$ for the reaction involving a Cpd I mimic, whereas an entropy-controlled process was suggested for the oxidation of the same substrate by a nonheme oxoiron(IV) species.[17,51]

A comparable contribution from the activation entropy and activation enthalpy to the free Gibbs activation energy found for the oxidation reactions by the Cpd I mimic indicates that the impact of these two terms on $\Delta G^{\ddagger}$ strongly depends on the temperature. Significantly, the oxidation of 4-Mb-alc and 4-Mb-ald by the Cpd I mimic becomes clearly entropy-controlled within the range of physiological temperatures (the $-T\Delta S^{\ddagger}$ term exceeds the $\Delta H^{\ddagger}$ term already above 5 and 27 °C for the oxidation of 4-Mb-alc and 4-Mb-ald, respectively), whereas the oxidation of the same substrates but with involvement of the Cpd II mimic remains an enthalpy-controlled process in the same temperature range.

The above considerations nicely underline the conclusions drawn from studies by Takahashi et al.,[13] which revealed a large contribution of the entropy term for the allylic hydroxylation reaction, indicating that $\Delta G^{\ddagger}$ rather than E_a should be used to predict the reaction mechanism. Thus, the above experimental work clearly points out that the theoretical approach in which the reaction mechanism and chemoselectivity are discussed on the basis of E_a and ipso facto neglecting the entropic contribution to the free energy of activation,[9,10,12] may indeed sometimes lead to inappropriate conclusions, especially when the considered oxidation reaction is characterized by a significant contribution of the entropy term to $\Delta G^{\ddagger}$. On the other hand, one should keep in mind that in the case of enzymatic reactions the entropic contribution to $\Delta G^{\ddagger}$ coming from the loss of rotational and translational degrees of freedom in the transition state is diminished by water molecules leaving the active pocket upon substrate entrance. Consequently, the entropic term in enzymatic reactions may even be lower than that in bimolecular reactions involving model systems without the protein environment.[52,53]

It has been shown that for C−H abstraction reactions a linear correlation of the energy barriers with the C−H bond energy (BDE_{C-H}), as well as with the energy of the newly formed O−H bond, can be expected.[54] A recent theoretical study revealed that a much better correlation can be found between calculated activation barriers and bond strengths (D_{C-H}) than BDE_{C-H}. The bond strength quantity is defined as a combination of BDE_{C-H} and the relaxation energy of the substrate radical ($RE_R^{\bullet}$), $D_{C-H} = BDE_{C-H} + |RE_R^{\bullet}|$.[34] This finding indicates that substrates that are characterized by comparable BDE_{C-H} values may display significantly different energy barriers for the transition state if they strongly differ in $RE_R^{\bullet}$. C−H abstraction from the selected aldehyde and alcohol represent such a case. While hydrogen abstraction from the aldehyde is associated with a rather minor structural reorganization in the transition state due to its planar geometry (sp^2 CHO), α-C−H abstraction from alcohol is characterized by significant $RE_R^{\bullet}$ arising from alteration of the tetrahedral arrangement (sp^3 α-C) to a planar arrangement during formation of the transition state. However, in the present study, no clear correlation between the calculated C−H bond energy (or D_{C-H}) and log(k/n) (where k is the reaction rate constant and n the number of abstractable hydrogen atoms) could be found (see Table 1) as a consequence of different contributions of the enthalpy and entropy terms to the overall $\Delta G^{\ddagger}$ for particular substrate oxidation reactions.

Especially, the $\Delta H^{\ddagger}$ values determined for the oxidation of 1-PhEtOH by both the Cpd I and II mimics are significantly larger than those for the oxidation of 4-Mb-alc, whereas the D_{C-H} values calculated for these two alcohols are rather very close. It is assumed that formation of the transition state in the

dx.doi.org/10.1021/ic402567h | Inorg. Chem. 2014, 53, 2848−2857

case of the oxidation of 1-PhEtOH (breakage of the C−H bond and formation of a new O−H bond) should reflect not only electronic but also steric effects. The latter can be ascribed to the steric hindrance of the methyl group in the neighborhood of the hydrogen atom to be abstracted, which leads to limited access of the more bulky alcohol to the iron oxo center. These effects, together with the fact that 1-PhEtOH does not possess an electron-donating group in the para position of the benzyl group, give a reason for considerably lower reactivity of this substrate in comparison to that of 4-MB-alc (ca. 35- and 5-fold smaller values of k were found for the oxidation reaction of 1-PhEtOH involving the Cpd I and Cpd II mimics, respectively).

The negative $\Delta S^{\ddagger}$ values for both oxidizing species are typical for bimolecular reactions and reflect a loss of translational and rotational degrees of freedom in the transition state. A comparison of the $\Delta S^{\ddagger}$ values determined for the oxidation of selected substrates by particular oxidizing species shows that they do not differ meaningfully. However, the general contribution of the activation entropy to the free activation energy for the reaction of the Cpd I mimic with selected substrates is much larger than that for the corresponding reactions involving the Cpd II mimic. The much more negative activation entropy for the substrate oxidation by the Cpd I mimic indicates higher order in the transition state, which points to a specific orientation of the substrate toward the iron oxo center. Both alcohols and aldehydes have a substantial dipole moment because of the polarized O−H and C═O bonds, respectively. The presence of a hydroxyl or carbonyl group may result in an orientation of the molecules with partially negatively charged oxygen atoms toward the very positive iron center. This effect is expected to have a larger impact on the reactions of the Cpd I mimic, which possesses the higher positive charge [formally an iron(V) center], than on the reactions involving the Cpd II mimic with an iron(IV) center. This effect may be reflected in the large difference in $\Delta S^{\ddagger}$ for the Cpd I and II mimics.

Further mechanistic insight into the C−H abstraction reactions by the selected Cpd I and II models can be gained from analysis of the pressure effects on the processes occurring in the transition state, i.e., breakage of the substrate C−H bond and formation of a new O−H bond. The activation volumes reported in Table 1 reveal slightly negative values of $\Delta V^{\ddagger}$ for the reactions of the Cpd I mimic but positive values for the reactions of the Cpd II mimic. Thus, the trend observed in the values of the activation volumes for the reactions with the Cpd I and II mimics nicely parallels the trend observed in the corresponding activation entropy data. Within the consensus of the hydrogen-atom-transfer mechanism, the high-valent iron oxo species abstracts hydrogen from the substrate to form a protonated, one-electron-reduced form of the oxidant and radical substrate intermediate. Considering C−H abstraction reactions involving the same substrate but two different oxidizing species, i.e., Cpd I and II mimics, the events accompanying formation of the transition state not only are determined by the electron affinity (EA) of the oxidant but also are related to the proton affinity of the hypothetical one-electron-reduced species formed after electron transfer. This is in agreement with experimental[55,56] and theoretical[57] studies, which clearly demonstrated that the strength of the O−H bond formed during hydrogen abstraction by Cpd I mimics not only reflects the EA term but also correlates well with a change in the basicity (pK_a) of the one-electron-reduced species. Although in the present study we consider hydrogen abstraction reactions involving two oxidizing species characterized by very different EAs, which dramatically affects their reactivity, detailed analysis of the volume changes on going from the reactant to the transition state provides insight into the effects discussed above. Thus, the substrate oxidation reactions by the Cpd II mimic are all accompanied by significantly positive activation volumes that vary between +10 and +17 $cm^3\ mol^{-1}$. Such values are very typical for rate-determining bond cleavage processes involving, for instance, homolysis of a C−H bond.[58] Formation of the transition state with involvement of the Cpd II mimic is associated with the partial transfer of one electron from the substrate into the higher-lying iron $d\pi^*$ orbitals, which leads to a change in the iron valence state to Fe^{III} and is expected to be associated with a volume increase.[58] The latter process is accompanied by the partial formation of an O−H bond, which, in principle, should make a negative contribution to the overall activation volume. However, taking into consideration that protonation of the one-electron-reduced species [oxoiron(III) porphyrin with a hydroxy axial ligand] must be a very fast process, it is reasonable to assume that the volume decrease due to formation of the O−H bond should have only a small impact on the overall volume changes in the transition state. In addition, a volume decrease that accompanies formation of an O−H bond can also be partially canceled by the volume increase associated with labilization of the hydroxy axial ligand in the position trans to the newly formed O−H bond because formation of Fe^{III}(TMPS) species with two strongly bound anionic ligands (HO^- axial ligands) seems to be very unlikely.[23,37] Thus, C−H bond homolysis coupled to reduction of the metal center in the Cpd II mimic is the most likely explanation for the significantly positive activation volumes found for reactions involving this oxidizing species.

The activation volumes reported for substrate oxidation by the Cpd I mimic are significantly more negative (ca. -2 ± 1 $cm^3\ mol^{-1}$) than those found for the $[(TMPS)Fe^{IV}{=}O(OH)]^{5-}$ complex. In contrast to the oxidation reactions catalyzed by the Cpd II mimic, formation of the transition state with involvement of the Cpd I mimic is associated with transfer of the substrate's electron to the low-lying singly occupied a_{2u} porphyrin orbital (porphyrin "hole" serving as an electronic sink), and there is no formal change in the iron valence state and, thus, no volume changes associated with this process. Protonation of the one-electron-reduced Cpd I, which still remains as the oxoferryl species, is assumed to proceed not as straightforward as in the case of protonation of the one-electron-reduced Cpd II, which could indicate that O−H bond formation plays an important role. Such bond formation in the second coordination sphere could indeed be in line with the small negative activation volumes found for these reactions. Alternatively, the data could point to a concerted bond formation/bond cleavage process, in which volume changes associated with both reaction components upon going to the transition state partially cancel to result in the overall slightly negative activation volumes found for these reactions. In this respect, the significantly positive activation volumes found for the reactions with the Cpd II mimic would, in turn, favor a stepwise mechanism in which first rate-determining bond cleavage is followed by fast O−H bond formation.

It should be kept in mind that electrostriction effects can also contribute to interpretation of the activation volume data. For instance, upon going from the reactant to the product state (formation of a protonated one-electron-reduced form of the

dx.doi.org/10.1021/ic402567h | Inorg. Chem. 2014, 53, 2848−2857

oxidant and radical substrate intermediate), there will be an overall change in the charge from 5− to 4− [including elimination of the trans HO ligand following protonation of $(P)Fe^{III}{=}O(OH)$] for the Cpd II reaction and no change in the charge for the Cpd I reaction (from 3− to 3−). Thus, electrostriction effects could play a role in the reactions of Cpd II (positive contribution to the overall volume changes), whereas they seem to be negligible for the reactions of Cpd I. This is in line with our results from the pressure-dependent measurements.

CONCLUSIONS

Model complexes of two highly reactive intermediates in the catalytic cycle of heme enzymes, viz., Cpds I and II, have successfully been stabilized in aqueous solution. This enabled for the first time examination of the pressure effects on the C−H abstraction reactions involving Cpd I and II mimics as oxidizing species. The detailed comparative studies of the reactivity of the latter species toward selected substrates revealed that the oxidation rate constant depends on both the chemical nature of the substrates and the type of reactive intermediate. Combined temperature and pressure measurements provided additional valuable information to comprehend the mechanistic aspects that affect the reactivity of Cpd I and II mimics and allowed us to draw the following conclusions: (i) Within the range of room and physiological temperatures, the oxidation of 4-Mb-alc and 4-Mb-ald by the Cpd II mimic is clearly an enthalpy-controlled process, whereas the oxidation of the same substrates by the Cpd I mimic becomes an entropy-controlled reaction. (ii) The oxidation reactions of the more bulky alcohol, 1-PhEtOH, which does not possess an electron-donating group in the para position of the benzyl group, are enthalpy-controlled under ambient conditions, independent of the oxidizing species used, i.e., Cpd I or II mimic. (iii) Different contributions of the enthalpy and entropy terms to the overall $\Delta G^{\ddagger}$ value for particular substrate oxidation reactions are reflected in the fact that no clear correlation between $\log(k/n)$ and the calculated C−H bond energy (or D_{C-H}) could be found in the present study. (iv) The significantly positive values of the activation volume found for the oxidation reactions involving the Cpd II mimic indicate that formation of the transition state by this oxidizing species is dominated by C−H bond homolysis processes coupled to reduction of the metal center, whereas formation of the H−O bond is suggested to play an important role in the transition state of the oxidation process involving participation of the Cpd I mimic. This is the most likely explanation for the small negative values of the activation volume found for reactions involving this oxidizing species.

ASSOCIATED CONTENT

Supporting Information

UV−vis spectral changes observed upon reaction of 4-MB-alc with $(TMPS^{\bullet+})Fe^{IV}{=}O$ and $(TMPS)Fe^{IV}{=}O(OH)$ and rate constants for the oxidation of selected substrates by Cpd I and II mimics as a function of the concentration, temperature, and pressure. This material is available free of charge via the Internet at http://pubs.acs.org.

AUTHOR INFORMATION

Corresponding Authors

*E-mail: stochel@chemia.uj.edu.pl.

*E-mail: vaneldik@chemie.uni-erlangen.de.

Notes

The authors declare no competing financial interest.

ACKNOWLEDGMENTS

This work was supported by the International Ph.D. Study Program at the Faculty of Chemistry, Jagiellonian University, within the Foundation for Polish Science MPD Program cofinanced by the European Regional Development Fund (MO). Support from the National Science Center (Grant 2012/05/B/STS/00389) is gratefully acknowledged. A.F. and R.v.E. gratefully acknowledge continued financial support from the Deutsche Forschungsgemeinschaft. This work was carried out with equipment purchased through financial support from the European Regional Development Fund in the framework of the Polish Innovation Economy Operational Program (Contract POIG.02.01.00-12-023/08). A.D.-M. acknowledges financial support from the Leading National Research Centre KNOW through the Marian Smoluchowski Scientific Consortium, Krakow, Poland.

REFERENCES

(1) Gross, Z.; Nimri, S.; Barzilay, C. M.; Simkhovich, L. *J. Biol. Inorg. Chem.* **1997**, *2*, 492.
(2) Nam, W.; Park, S.-E.; Lim, I. K.; Lim, M. H.; Hong, J.; Kim, J. *J. Am. Chem. Soc.* **2003**, *125*, 14672.
(3) Song, W. J.; Ryu, Y. O.; Song, R.; Nam, W. *J. Biol. Inorg. Chem.* **2005**, *10*, 294.
(4) Groves, J. T.; Subramanian, D. V. *J. Am. Chem. Soc.* **1984**, *106*, 2177.
(5) Groves, J. T.; Nemo, T. E. *J. Am. Chem. Soc.* **1983**, *105*, 5786.
(6) Yang, S. J.; Nam, W. *Inorg. Chem.* **1998**, *37*, 606.
(7) Ohno, T.; Suzuki, N.; Dokoh, T.; Urano, Y.; Kikuchi, K.; Hirobe, M.; Higuchi, T.; Nagano, T. *J. Inorg. Biochem.* **2000**, *82*, 123.
(8) De Visser, S. P. *J. Biol. Inorg. Chem.* **2006**, *11*, 168.
(9) De Visser, S. P.; Ogliaro, F.; Sharma, P. K.; Shaik, S. *Angew. Chem., Int. Ed.* **2002**, *41*, 1947.
(10) De Visser, S. P.; Ogliaro, F.; Sharma, P. K.; Shaik, S. *J. Am. Chem. Soc.* **2002**, *124*, 11809.
(11) Shaik, S.; Kumar, D.; de Visser, S. P.; Altun, A.; Thiel, W. *Chem. Rev.* **2005**, *105*, 2279.
(12) Shaik, S.; Cohen, S.; Wang, Y.; Chen, H.; Kumar, D.; Thiel, W. *Chem. Rev.* **2010**, *110*, 949.
(13) Takahashi, A.; Kurahashi, T.; Fujii, H. *Inorg. Chem.* **2007**, *46*, 6227.
(14) Fertinger, C.; Franke, A.; van Eldik, R. *J. Biol. Inorg. Chem.* **2012**, *17*, 27.
(15) Finn, M.; Friedline, R.; Suleman, N. K.; Wohl, C. J.; Tanko, J. M. *J. Am. Chem. Soc.* **2004**, *126*, 7578.
(16) Sherry, A. E.; Wayland, B. B. *J. Am. Chem. Soc.* **1990**, *112*, 1259.
(17) Oh, N. Y.; Suh, Y.; Park, M. J.; Seo, M. S.; Kim, J.; Nam, W. *Angew. Chem., Int. Ed.* **2005**, *44*, 4235.
(18) Nam, W.; Lim, M. H.; Lee, H. J.; Kim, C. *J. Am. Chem. Soc.* **2000**, *122*, 6641.
(19) Nam, W.; Jin, S. W.; Lim, M. H.; Ryu, J. Y.; Kim, C. *Inorg. Chem.* **2002**, *41*, 3647.
(20) Nam, W.; Lim, M. H.; Moon, S. K.; Kim, C. *J. Am. Chem. Soc.* **2000**, *122*, 10805.
(21) Kang, Y.; Chen, H.; Jeong, Y. J.; Lai, W.; Bae, E. H.; Shaik, S.; Nam, W. *Chem.—Eur. J.* **2009**, *15*, 10039.
(22) Kumar, D.; Tahsini, L.; de Visser, S. P.; Kang, H. Y.; Kim, S. J.; Nam, W. *J. Phys. Chem. A* **2009**, *113*, 11713.
(23) Wolak, M.; van Eldik, R. *Chem.—Eur. J.* **2007**, *13*, 4873.
(24) Liu, M.; Su, Y. O. J. *Electroanal. Chem.* **1998**, *452*, 113.
(25) Oszajca, M.; Drzewiecka-Matuszek, A.; Franke, A.; Rutkowska-Żbik, D.; Brindell, M.; Witko, M.; Stochel, G.; van Eldik, R. *Chem.—Eur. J.*, 10.1002/chem.201303694.

(26) van Eldik, R.; Palmer, D. A.; Schmidt, R.; Kelm, H. *Inorg. Chim. Acta* **1981**, *50*, 131.
(27) van Eldik, R.; Gaede, W.; Wieland, S.; Kraft, J.; Spitzer, M.; Palmer, D. A. *Rev. Sci. Instrum.* **1993**, *64*, 1355.
(28) Dirac, P. A. M. *Proc. R. Soc. London* **1929**, *123*, 714.
(29) Slater, J. C. *Phys. Rev.* **1951**, *81*, 385.
(30) Vosko, S. H.; Wilk, L.; Nusair, M. *Can. J. Phys.* **1980**, *58*, 1200.
(31) Becke, A. D. *J. Chem. Phys.* **1993**, *98*, 5648.
(32) Becke, A. D. *Phy. Rev. A* **1988**, *38*, 3098.
(33) Lee, C.; Yang, W.; Parr, R. G. *Phys. Rev. B* **1988**, *37*, 785.
(34) Shaik, S.; Kumar, D.; de Visser, S. P. *J. Am. Chem. Soc.* **2008**, *130*, 10128.
(35) *TURBOMOLE*, version 6.3; TURBOMOLE GmbH saf, Forschungszentrum Karlsruhe, Karlsruhe, Germany, 2011.
(36) Laverman, L. E.; Ford, P. C. *J. Am. Chem. Soc.* **2001**, *123*, 11614.
(37) Wolak, M.; van Eldik, R. *J. Am. Chem. Soc.* **2005**, *127*, 13312.
(38) Nam, W.; Choi, H. J.; Han, H. J.; Cho, S. H.; Lee, H. J.; Han, S.-Y. *Chem. Commun.* **1999**, 387.
(39) Franke, A.; Fertinger, C.; van Eldik, R. *Angew. Chem., Int. Ed.* **2008**, *47*, 5238.
(40) Fertinger, C.; Hessenauer-Ilicheva, N.; Franke, A.; van Eldik, R. *Chem.—Eur. J.* **2009**, *15*, 13435.
(41) Pan, Z.; Newcomb, M. *Inorg. Chem.* **2007**, *46*, 6767.
(42) Pestovsky, O.; Bakac, A. *J. Am. Chem. Soc.* **2004**, *126*, 13757.
(43) Bell, S. R.; Groves, J. T. *J. Am. Chem. Soc.* **2009**, *131*, 9640.
(44) Koshino, N.; Saha, B.; Espenson, J. H. *J. Org. Chem.* **2003**, *68*, 9364.
(45) Dolphin, D.; Traylor, T. G.; Xie, L. Y. *Acc. Chem. Res.* **1997**, *30*, 251.
(46) Fujii, H. *J. Am. Chem. Soc.* **1993**, *115*, 4641.
(47) Fujii, H.; Kurahashi, T.; Tosha, T.; Yoshimura, T.; Kitagawa, T. *J. Inorg. Biochem.* **2006**, *100*, 533.
(48) Seok, W. K.; Meyer, T. J. *Inorg. Chem.* **2005**, *44*, 3931.
(49) Groves, J. T.; McClusky, G. A.; White, R. E.; Coon, M. J. *Biochem. Biophys. Res. Commun.* **1978**, *81*, 154.
(50) Shaik, S.; de Visser, S. P.; Ogliaro, F.; Schwarz, H.; Schröder, D. *Curr. Opin. Chem. Biol.* **2002**, *6*, 556.
(51) The values of the activation entropy cited in ref 17 were recalculated based on the k_{on} values reported in Table 1 (ref 17) using the Eyring equation.
(52) Page, M. I.; Jenck, W. P. *Proc. Natl. Acad. Sci. U.S.A.* **1971**, *68*, 1678.
(53) Shaik, S.; Hirao, H.; Kumar, D. *Acc. Chem. Res.* **2007**, *40*, 532.
(54) Mayer, J. M. *Acc. Chem. Res.* **1998**, *31*, 441.
(55) Prokop, K. A.; de Visser, S. P.; Goldberg, D. P. *Angew. Chem., Int. Ed.* **2010**, *49*, 5091.
(56) Green, M. T.; Dawson, J. H.; Gray, H. B. *Science* **2004**, *304*, 1653.
(57) Kumar, D.; Sastry, G. N.; de Visser, S. P. *J. Phys. Chem. B* **2012**, *116*, 718.
(58) van Eldik, R.; Asano, T.; le Noble, W. J. *Chem. Rev.* **1989**, *89*, 549.